

η' and η mesons at high T when the $U_A(1)$ and chiral symmetry breaking are tied

Horvatić, Davor; Kekez, Dalibor; Klabučar, Dubravko

Source / Izvornik: **Physical Review D**, 2019, 99

Journal article, Published version

Rad u časopisu, Objavljena verzija rada (izdavačev PDF)

<https://doi.org/10.1103/PhysRevD.99.014007>

Permanent link / Trajna poveznica: <https://um.nsk.hr/um:nbn:hr:217:336024>

Rights / Prava: [In copyright](#) / [Zaštićeno autorskim pravom](#).

Download date / Datum preuzimanja: **2024-07-15**



Repository / Repozitorij:

[Repository of the Faculty of Science - University of Zagreb](#)



η' and η mesons at high T when the $U_A(1)$ and chiral symmetry breaking are tied

Davor Horvatić,¹ Dalibor Kekez,² and Dubravko Klabučar¹

¹*Physics Department, Faculty of Science, University of Zagreb, Bijenička cesta 32, 10000 Zagreb, Croatia*

²*Rugjer Bošković Institute, Bijenička cesta 34, 10000 Zagreb, Croatia*



(Received 16 October 2018; published 9 January 2019)

The approach to the η' - η complex employing chirally well-behaved quark-antiquark bound states and incorporating the non-Abelian axial anomaly of QCD through the generalization of the Witten-Veneziano relation is extended to finite temperatures. Employing the chiral condensate has led to a sharp chiral and $U_A(1)$ symmetry restoration, but with the condensates of quarks with realistic explicit chiral symmetry breaking—which exhibit a smooth, crossover chiral symmetry restoration in qualitative agreement with lattice QCD results—we get a crossover $U_A(1)$ transition with a smooth and gradual melting of anomalous mass contributions. In this way, we obtain a substantial decrease in the η' mass around the chiral transition temperature, but no decrease in the η mass. This is consistent with current empirical evidence.

DOI: 10.1103/PhysRevD.99.014007

I. INTRODUCTION

The experiments at heavy-ion collider facilities—such as RHIC, LHC, FAIR, and NICA—aim to produce a new form of hot and/or dense QCD matter [1,2]. Clear signatures of its production are thus very much needed. The most compelling such signal would be a change in the pertinent symmetries, i.e., the restoration (in hot and/or dense matter) of the symmetries of the QCD Lagrangian which are broken in the vacuum, notably the $[SU_A(N_f)$ flavor] chiral symmetry for $N_f = 3 = 2 + 1$ light quark flavors q , and the $U_A(1)$ symmetry. This provides much motivation to establish that experiment indeed shows this, as well as to give theoretical explanations of such phenomena.

The first signs of a (partial) restoration of the $U_A(1)$ symmetry were claimed to be seen in 200 GeV Au + Au collisions [3,4] at RHIC by Csörgő *et al.* [5]. They analyzed the η' -meson data of the PHENIX [3] and STAR [4] collaborations through several models for hadron multiplicities, and found that the η' mass ($M_{\eta'} = 957.8$ MeV in vacuum) decreases by at least 200 MeV inside the fireball. The vacuum η' is, comparatively, so very massive since it is predominantly the $SU_V(N_f)$ -flavor singlet state η_0 . Its mass M_{η_0} receives a sizable anomalous contribution ΔM_{η_0} due to the $U_A(1)$ symmetry violation by the non-Abelian axial Adler-Bell-Jackiw anomaly [“gluon anomaly,” or

“ $U_A(1)$ anomaly” for short], which makes the divergence of the singlet axial quark current $\bar{q}\gamma^\mu\gamma_5\frac{1}{2}\lambda^0q$ nonvanishing even in the chiral limit of vanishing current masses of quarks, $m_q \rightarrow 0$. This mass decrease is then a sign of a *partial* $U_A(1)$ symmetry restoration in the sense of a diminishing contribution of the $U_A(1)$ anomaly to the η' mass, which would decrease to a value readily understood in the same way [6] as the masses of the octet of the light pseudoscalar mesons $P = \pi^{0,\pm}$, $K^{0,\pm}$, \bar{K}^0 , η , which are exceptionally light almost-Goldstone bosons of dynamical chiral symmetry breaking (DChSB).

A recent experimental paper studied 200 GeV Au + Au collisions [7]. Although a new analysis of the limits on the η' and η masses was beyond the scope of Ref. [7], the data contained therein make it possible, and preliminary considerations [8] confirm the findings of Ref. [5].

The first explanation [9] of these original findings [5] was offered by conjecturing that the Yang-Mills (YM) topological susceptibility, which leads to the anomalously high η' mass, should be viewed through the Leutwyler-Smilga (LS) [10] relation (12). This ultimately implies that the anomalous part of the η' mass decreases together with the quark-antiquark ($q\bar{q}$) chiral-limit condensate $\langle\bar{q}q\rangle_0(T)$ as the temperature T grows towards the chiral restoration temperature T_{Ch} and beyond. This connection between the $U_A(1)$ symmetry restoration and the chiral symmetry restoration was just a conjecture until our more recent paper [11] strengthened the support for this scenario. Nevertheless, there was also a weakness: our approach predicted the decrease of not only the η' mass, but also an even more drastic decrease of the η mass M_η , and signs for that have not been seen in any currently available data [7,12]. In the present paper, we show that the predicted

Published by the American Physical Society under the terms of the [Creative Commons Attribution 4.0 International license](https://creativecommons.org/licenses/by/4.0/). Further distribution of this work must maintain attribution to the author(s) and the published article's title, journal citation, and DOI. Funded by SCOAP³.

decrease of M_η [9] was the consequence of employing the chiral-limit condensate $\langle \bar{q}q \rangle_0(T)$, since it decreases too fast with T after approaching $T \sim T_{\text{Ch}}$. We then perform $T > 0$ calculations in the framework of the more recent work by Benić *et al.* [11], where the LS relation (12) is replaced by the full-QCD topological charge parameter (18) [13–15]. There, one can employ $q\bar{q}$ condensates for realistically massive u , d , and s quarks, with a much smoother T dependence. As a result, the description of the η - η' complex of Ref. [9] is significantly improved, since our new T dependences of the pseudoscalar meson masses do not exhibit a decrease of the η mass, while a considerable decrease of the η' mass still exists, which is consistent with the empirical findings [5].

II. A SURVEY OF THE η - η' COMPLEX

The light pseudoscalar mesons are simultaneously $q\bar{q}'$ bound states ($q, q' = u, d, s$) and (almost-)Goldstone bosons of the DChSB of nonperturbative QCD. We can implement both simultaneously by using the Dyson-Schwinger (DS) equations as Green functions of QCD (see, e.g., Refs. [16–19] for reviews). Particularly pertinent are the gap equation for *dressed* quark propagators $S_q(p)$ with DChSB-generated self-energies $\Sigma_q(p)$,

$$S_q^{-1}(p) = S_q^{\text{free}}(p)^{-1} - \Sigma_q(p), \quad (q = u, d, s), \quad (1)$$

(while S_q^{free} are free ones), and the Bethe-Salpeter equation (BSE) for the $q\bar{q}'$ meson bound-state vertices $\Gamma_{q\bar{q}'}$,

$$\Gamma_{q\bar{q}'}(k, p)_{ef} = \int \left[S_q \left(\ell + \frac{p}{2} \right) \Gamma_{q\bar{q}'}(\ell, p) S_{q'} \left(\ell - \frac{p}{2} \right) \right]_{gh} \times K(k - \ell)_{ef}^{hg} \frac{d^4 \ell}{(2\pi)^4}, \quad (2)$$

where K is the interaction kernel, and e, f, g, h represent (schematically) the collective spinor, color, and flavor indices.

This nonperturbative and covariant bound-state DS approach can be applied for various degrees of truncations, assumptions, and approximations, ranging from *ab initio* QCD calculations and sophisticated truncations (see, e.g., Refs. [16–22] and references therein) to very simplified modeling of hadron phenomenology, such as utilizing Nambu–Jona-Lasinio point interactions. For applications in involved contexts such as nonzero temperature or density, strong simplifications are especially needed for tractability. This is why the separable approximation [23] is adopted in this paper [see the discussion between Eqs. (4) and (5)]. However, when describing pseudoscalar mesons (including η and η') reproducing the correct chiral behavior of QCD is much more important than the dynamics-dependent details of their internal bound-state structure.

A rarity among bound-state approaches, the DS approach can also achieve the correct QCD chiral behavior regardless of the details of model dynamics, but under the condition of a consistent truncation of DS equations, respecting pertinent Ward-Takahashi identities [16–19]. A consistent DS truncation, where DChSB is very well understood, is the rainbow-ladder approximation (RLA). Since it also enables tractable calculations, it is still the most used approximation in phenomenological applications, and we also adopt it here. In the RLA, the BSE (2) employs the dressed quark propagator solution $S(p)$ from the gap equation (1) and (4), which in turn employs the same effective interaction kernel as the BSE. It has a simple gluon-exchange form, where both quark-gluon vertices are bare,

$$[K(k)]_{ef}^{hg} = ig^2 D_{\mu\nu}^{ab}(k)_{\text{eff}} \left[\frac{\lambda^a}{2} \gamma^\mu \right]_{eg} \left[\frac{\lambda^b}{2} \gamma^\nu \right]_{hf}, \quad (3)$$

so that the quark self-energy in the gap equation is

$$\Sigma_q(p) = - \int \frac{d^4 \ell}{(2\pi)^4} g^2 D_{\mu\nu}^{ab}(p - \ell)_{\text{eff}} \frac{\lambda^a}{2} \gamma^\mu S_q(\ell) \frac{\lambda^b}{2} \gamma^\nu, \quad (4)$$

where $D_{\mu\nu}^{ab}(k)_{\text{eff}}$ is an effective gluon propagator.

These simplifications should be compensated by modeling the effective gluon propagator $D_{\mu\nu}^{ab}(k)_{\text{eff}}$ in order to reproduce well the relevant phenomenology; here, pseudoscalar (P) meson masses M_P , decay constants f_P , and condensates $\langle \bar{q}q \rangle$, including T -dependence of all these. In the present paper, we use the same model as in Ref. [9] and attempt to improve their approach to the T dependence of the $U_A(1)$ anomaly. All of the details on the functional form and parameters of this model interaction can be found in the Sec. II A of Ref. [24]. Such models—so-called rank-2 separable models—are phenomenologically successful (see, e.g., Refs. [23–27]). However, they have the well-known drawback of predicting a somewhat too low transition temperature: the model we use in this paper and that was used in Refs. [9,24,26,27] has $T_{\text{Ch}} = 128$ MeV, i.e., some 17% below the now widely accepted central value of 154 ± 9 MeV [28–30]. But, rather than quantitative predictions at specific absolute temperatures, we are interested in the relative connection between the chiral restoration temperature T_{Ch} and the temperature scales characterizing signs of the effective disappearance of the $U_A(1)$ anomaly, for which the present model is adequate. In addition, Ref. [31] showed that coupling to the Polyakov loop can increase T_{Ch} , while the qualitative features of the T dependence of the model are preserved. Thus, separable model results at $T > 0$ are most meaningfully presented as functions of the relative temperature T/T_{Ch} , as in Refs. [9,24].

Anyway, regardless of the details of the model dynamics [i.e., the choice of $D_{\mu\nu}^{ab}(k)_{\text{eff}}$] and thanks to the consistent truncation of DS equations, the BSE (2) yields the masses

$M_{q\bar{q}'}$ of pseudoscalar $P \sim q\bar{q}'$ mesons which satisfy the Gell-Mann–Oakes–Renner-type relation with the current masses $m_q, m_{q'}$ of the corresponding quarks:

$$M_{q\bar{q}'}^2 = \text{const}(m_q + m_{q'}), \quad (q, q' = u, d, s). \quad (5)$$

While this guarantees that all $M_{q\bar{q}'} \rightarrow 0$ in the chiral limit, it also shows that the RLA cannot lead to any $U_A(1)$ -anomalous contribution responsible for ΔM_{η_0} . That is, the RLA gives us only the nonanomalous part \hat{M}_{NA}^2 of the squared-mass matrix $\hat{M}^2 = \hat{M}_{NA}^2 + \hat{M}_A^2$ of the hidden-flavor ($q = q'$) light ($q = u, d, s$) pseudoscalar mesons. In the basis $\{u\bar{u}, d\bar{d}, s\bar{s}\}$, \hat{M}_{NA}^2 is simply $\hat{M}_{NA}^2 = \text{diag}[M_{u\bar{u}}^2, M_{d\bar{d}}^2, M_{s\bar{s}}^2]$. The anomalous part \hat{M}_A^2 arises because the pseudoscalar hidden-flavor states $q\bar{q}$ are not protected from the flavor-mixing QCD transitions (through anomaly-dominated pseudoscalar gluonic intermediate states), as depicted in Fig. 1. They are obviously beyond the reach of the RLA and horrendously hard to calculate. Nevertheless, they cannot be neglected, as can be seen in the Witten-Veneziano relation (WVR) [32,33], which remarkably relates the full-QCD quantities (η', η , the K -meson masses $M_{\eta', \eta, K}$, and the pion decay constant f_π) to the topological susceptibility χ_{YM} of the (pure-gauge) YM theory:

$$M_{\eta'}^2 + M_\eta^2 - 2M_K^2 = 2N_f \frac{\chi_{\text{YM}}}{f_\pi^2} = M_{U_A(1)}^2. \quad (6)$$

Its chiral-limit-nonvanishing rhs is large (roughly 0.8 to 0.9 GeV²), while Eq. (5) basically leads to the cancellation of all chiral-limit-vanishing contributions on the lhs [9]. The rhs is the WVR result for the total mass contribution of the $U_A(1)$ anomaly to the η - η' complex, $M_{U_A(1)}$.

The \hat{M}_A^2 matrix elements generated by the $U_A(1)$ -anomaly-dominated transitions $q\bar{q} \rightarrow q'\bar{q}'$ (see Fig. 1) can be written [35] in the flavor basis $\{u\bar{u}, d\bar{d}, s\bar{s}\}$ as

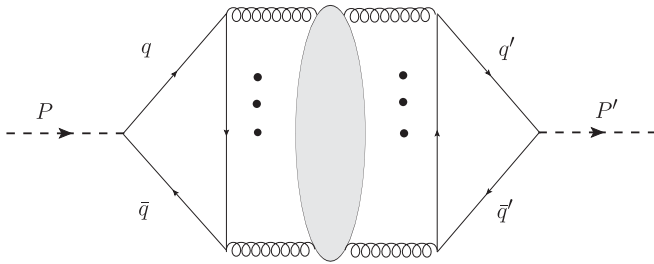


FIG. 1. Axial-anomaly-induced, flavor-mixing transitions from hidden-flavor pseudoscalar states $P = q\bar{q}$ to $P' = q'\bar{q}'$ including both possibilities $q = q'$ and $q \neq q'$. All lines and vertices are dressed. The gray blob symbolizes all possible intermediate states enabling this transition. The three bold dots symbolize an even [34] but otherwise unlimited number of additional gluons. As pointed out in Ref. [34], the diamond graph is just the simplest example of such a contribution.

$$\langle q\bar{q} | \hat{M}_A^2 | q'\bar{q}' \rangle = b_q b_{q'}, \quad (q, q' = u, d, s). \quad (7)$$

Here $b_q = \sqrt{\beta}$ for both $q = u, d$, since we assume $m_u = m_d \equiv m_l$ [i.e., isospin $SU(2)$ symmetry] which is an excellent approximation for most purposes in hadronic physics. For example, $M_{u\bar{u}} = M_{d\bar{d}} \equiv M_{l\bar{l}} = M_{u\bar{d}} \equiv M_\pi$ obtained from the BSE (2) is our RLA model pion mass for $\pi^+(\pi^-) = u\bar{d}(d\bar{u})$ and $\pi^0 = (u\bar{u} - d\bar{d})/\sqrt{2}$, so that $\hat{M}_{NA}^2 = \text{diag}[M_\pi^2, M_\pi^2, M_{s\bar{s}}^2]$. It still contains $M_{s\bar{s}}$, the mass of the unphysical (but theoretically very useful) $s\bar{s}$ pseudoscalar obtained in the RLA. However, thanks to Eq. (5), it can also be expressed through the masses of physical mesons, $M_{s\bar{s}}^2 = 2M_{u\bar{s}}^2 - M_{u\bar{d}}^2 = 2M_K^2 - M_\pi^2$, to a very good approximation [24,27,34–37]. Its decay constant $f_{s\bar{s}}$ is calculated in the same way as f_π and f_K .

Since the s quark is much heavier than the u and d quarks, in Eq. (7) we have $b_q = X\sqrt{\beta}$ for $q = s$, with $X < 1$. Transitions to and from more massive s quarks are suppressed, and the quantity X expresses this influence of the $SU(3)$ flavor symmetry breaking. The most common choice for the flavor-breaking parameter has been the estimate $X = f_\pi/f_{s\bar{s}}$ [9,24,27,34–37], but we found [11] that it necessarily arises in the variant of our approach relying on Shore’s generalization of the WVR (6) [13,14] (see Sec. III).

The anomalous mass matrix \hat{M}_A^2 [which is of the pairing form (7) in the hidden-flavor basis $\{u\bar{u}, d\bar{d}, s\bar{s}\}$ in the octet-singlet basis $\{\pi^0, \eta_8, \eta_0\}$ of hidden-flavor pseudoscalars becomes

$$\hat{M}_A^2 = \beta \begin{bmatrix} 0 & 0 & 0 \\ 0 & \frac{2}{3}(1-X)^2 & \frac{\sqrt{2}}{3}(2-X-X^2) \\ 0 & \frac{\sqrt{2}}{3}(2-X-X^2) & \frac{1}{3}(2+X)^2 \end{bmatrix}, \quad (8)$$

which shows that the $SU(3)$ flavor breaking [$X \neq 1$] is necessary for the anomalous contribution to the η_8 mass squared, $\Delta M_{\eta_8}^2 = \beta(2/3)(1-X)^2$. In the flavor $SU(3)$ -symmetric case ($X = 1$), only the η_0 mass receives a $U_A(1)$ -anomaly contribution: $M_{U_A(1)}^2 = \Delta M_{\eta_0}^2 = 3\beta$ in this limit. Otherwise, $M_{U_A(1)}^2 \equiv \text{Tr} \hat{M}_A^2 = (2+X^2)\beta$.

The $SU(3)$ breaking ($X \neq 1$) causes \hat{M}_A^2 [Eq. (8)] to be off diagonal, but in this basis the $\{\eta_8, \eta_0\}$ submatrix of \hat{M}_{NA}^2 also gets strong, negative off-diagonal elements, $M_{80}^2 = \sqrt{2}(M_\pi^2 - M_{s\bar{s}}^2)/3$ (see, e.g., Ref. [35]). Equation (8) thus shows that the interplay of the flavor symmetry breaking ($X < 1$) with the anomaly is necessary for the partial cancellation of the off-diagonal (8,0) elements in the complete mass matrix $\hat{M}^2 = \hat{M}_{NA}^2 + \hat{M}_A^2$, i.e., to obtain the physical isoscalars in a rough approximation as $\eta \approx \eta_8$ and $\eta' \approx \eta_0$. How this changes with diminishing $U_A(1)$ -anomaly contributions is exhibited in Secs. IV and V.

Since the isospin-limit π^0 decouples from the anomaly and mixing, only the isoscalar-subspace 2×2 mass matrix

\hat{M}^2 needs to be considered. Even though \hat{M}^2 is strongly off diagonal in the isoscalar basis $\{\eta_{\text{NS}}, \eta_{\text{S}}\}$ (the NS-S basis),

$$\begin{bmatrix} \eta_{\text{NS}} \\ \eta_{\text{S}} \end{bmatrix} \equiv \begin{bmatrix} \frac{1}{\sqrt{2}}(u\bar{u} + d\bar{d}) \\ s\bar{s} \end{bmatrix} \equiv \begin{bmatrix} \frac{1}{\sqrt{3}} & \sqrt{\frac{2}{3}} \\ -\sqrt{\frac{2}{3}} & \frac{1}{\sqrt{3}} \end{bmatrix} \begin{bmatrix} \eta_8 \\ \eta_0 \end{bmatrix}, \quad (9)$$

in this basis it has the simple form

$$\hat{M}^2 \equiv \begin{bmatrix} M_{\text{NS}}^2 & M_{\text{NS S}}^2 \\ M_{\text{S NS}}^2 & M_{\text{S}}^2 \end{bmatrix} = \begin{bmatrix} M_{\pi}^2 + 2\beta & \sqrt{2}\beta X \\ \sqrt{2}\beta X & M_{s\bar{s}}^2 + \beta X^2 \end{bmatrix}, \quad (10)$$

which also shows that when the $U_A(1)$ -anomaly contributions vanish (i.e., $\beta \rightarrow 0$) the NS-S scenario is realized. This means that not only do the physical isoscalars become $\eta \rightarrow \eta_{\text{NS}}$ and $\eta' \rightarrow \eta_{\text{S}}$, but also that their respective masses become M_{π} and $M_{s\bar{s}}$.

Our experience with various dynamical models (at $T = 0$) shows [27,34–37] that after pions and kaons are correctly described, a good determination of the anomalous mass shift parameter is sufficient for Eq. (10) to give good η' and η masses, since $M_{s\bar{s}}^2 = 2M_K^2 - M_{\pi}^2$ holds well.

Nevertheless, calculating the anomalous contributions ($\propto \beta$) in DS approaches is a very difficult task. Reference [38] explored this by taking the calculation beyond the RLA, but they had to adopt extremely schematic model interactions (proportional to δ functions in momenta) for both the ladder-truncation part (3) and the anomaly-producing part. Another approach [39] obtained qualitative agreement with the lattice on χ_{YM} (and, consequently, acceptable masses for η' and η) by assuming that the contributions to Fig. 1 are dominated by the simplest one—the diamond graph—if it is appropriately dressed (in particular, by an appropriately singular quark-gluon vertex).

However, we take a different route, since our goal is *not* to figure out how the breaking of $U_A(1)$ comes about on a microscopic level, but rather to phenomenologically model and study the high- T behavior of the masses of the realistic η' and η , along with other light pseudoscalar mesons. In the DS context, the most suitable approach is then the one developed in Refs. [27,34–37] and extended to $T > 0$ in Refs. [9,24].

The key is that the $U_A(1)$ anomaly is suppressed in the limit of large number of QCD colors N_c [32,33]. So, in the sense of the $1/N_c$ expansion, it is a controlled approximation to view the anomaly contribution as a perturbation with respect to the (nonsuppressed) results obtained through the RLA (3)–(4). While considering meson masses, it is thus not necessary to look for anomaly-induced corrections to the RLA Bethe-Salpeter wave

functions,¹ which are consistent with DChSB and with the chiral QCD behavior (5) that is essential for describing pions and kaons. The breaking of nonet symmetry by the $U_A(1)$ anomaly can be introduced just at the level of the masses in the η' - η complex, by adding the anomalous contribution \hat{M}_A^2 to the RLA-calculated \hat{M}_{NA}^2 . Its anomaly mass parameter β can be obtained by fitting [34] the empirical masses of η and η' or, preferably, from lattice results on the YM topological susceptibility χ_{YM} (because then no new fitting parameters are introduced). Employing the WVR (6) yields [9,35] $\beta = \beta_{\text{WV}}$, while Shore's generalization gives (see Sec. III) $\beta = \beta_{\text{Sho}}$ [11],

$$\beta_{\text{WV}} = \frac{6\chi_{\text{YM}}}{(2 + X^2)f_{\pi}^2}, \quad \beta_{\text{Sho}} = \frac{2A}{f_{\pi}^2} \approx \frac{2\chi_{\text{YM}}}{f_{\pi}^2}, \quad (11)$$

where A is the QCD topological charge parameter, given below by Eq. (18) in terms of $q\bar{q}$ condensates of massive quarks, which turns out to be crucial for a realistic T dependence of the masses in the η' - η complex.

III. EXTENSION TO $T \geq 0$

Extending our treatment [27,34–37] of the $\eta' - \eta$ complex to $T > 0$ is clearly more complicated. Since to the best of our knowledge there is no systematic derivation of the $T > 0$ version of either the WVR (6) or its generalization by Shore [13,14], it is tempting to try to straightforwardly replace all quantities by their T -dependent versions. In the WVR, these are the full-QCD quantities $M_{\eta'}(T)$, $M_{\eta}(T)$, $M_K(T)$, and $f_{\pi}(T)$, but also $\chi_{\text{YM}}(T)$, which is a pure-gauge, YM quantity and thus much more resistant to high temperatures than QCD quantities that also contain quark degrees of freedom. Indeed, lattice calculations indicate that the decrease of $\chi_{\text{YM}}(T)$ (from which one would expect the decrease of the anomalous η' mass) only starts at a T some 100 MeV (or even more) above the (pseudo)critical temperature T_{Ch} for the chiral symmetry restoration of full QCD, near where decay constants already decrease appreciably. It was then shown [24] that the straightforward extension of the T dependence of the YM susceptibility would even predict an increase of the η' mass around and beyond T_{Ch} , contrary to experiment [5].

It could be expected that at high T , the original WVR (6) will not work since it relates the full-QCD quantities with a much more temperature-resistant YM quantity, $\chi_{\text{YM}}(T)$.

¹It is instructive to recall [36,40] that nonet symmetry (or a broken version thereof) is in fact assumed (explicitly or implicitly) by all approaches using the simple hidden-flavor basis $q\bar{q}$, e.g., to construct the $SU(3)$ pseudoscalar meson states η_0 and η_8 without distinguishing between the $q\bar{q}$ states belonging to the singlet and those belonging to the octet. An independent *a posteriori* support for our approach is also that η and $\eta' \rightarrow \gamma\gamma^{(*)}$ processes are described well [34–37].

However, this problem can be eliminated [9] by using, at $T = 0$, the (inverted) Leutwyler-Smilga (LS) relation [10]

$$\chi_{\text{YM}} = \frac{\chi}{1 + \chi \left(\frac{1}{m_u} + \frac{1}{m_d} + \frac{1}{m_s} \right) \frac{1}{\langle \bar{q}q \rangle_0}} \equiv \tilde{\chi} \quad (12)$$

to express χ_{YM} in the WVR (6) through the full-QCD topological susceptibility χ and the chiral-limit condensate $\langle \bar{q}q \rangle_0$. Thus the zero-temperature WVR is retained, while the full-QCD quantities in $\tilde{\chi}$ do not have the T dependence mismatch with the rest of Eq. (6). Thus, instead of $\chi_{\text{YM}}(T)$, Ref. [9] used the combination $\tilde{\chi}(T)$ [Eq. (12)] at $T > 0$, where the QCD topological susceptibility χ in the light-quark sector can be expressed as [10,15,41]

$$\chi = \frac{-1}{\left(\frac{1}{m_u} + \frac{1}{m_d} + \frac{1}{m_s} \right) \frac{1}{\langle \bar{q}q \rangle_0}} + \mathcal{C}_m. \quad (13)$$

This implies that the (partial) restoration of $U_A(1)$ symmetry is strongly tied to the chiral symmetry restoration, since it is not $\chi_{\text{YM}}(T)$ but rather $\langle \bar{q}q \rangle_0(T)$ [through $\tilde{\chi}(T)$] that determines the T dependence of the anomalous parts of the masses in the η - η' complex [9]. The dotted curve in Fig. 2 illustrates how $\langle \bar{q}q \rangle_0(T)$ decreases steeply to zero as $T \rightarrow T_{\text{Ch}}$, indicative of the second-order phase transition.

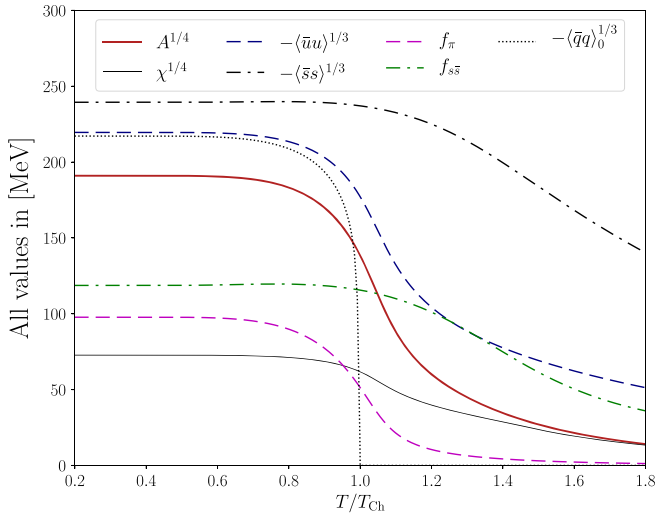


FIG. 2. The relative-temperature T/T_{Ch} dependences of the pertinent order parameters calculated in our usual [9,24] separable interaction model. The odd man out is the (third root of the absolute value of the) chiral condensate $\langle \bar{q}q \rangle_0(T)$, which decreases steeply at $T = T_{\text{Ch}}$ and dictates similar behavior [9] to $\tilde{\chi}(T)$. All of the other displayed quantities exhibit smooth, crossover behaviors, which are smoother for heavier flavors: the dash-dotted and dashed curves are the (third roots of the absolute values of the) condensates $\langle \bar{s}s \rangle(T)$ and $\langle \bar{u}u \rangle(T)$, respectively, the thin solid curve is the resulting topological susceptibility $\chi(T)^{1/4}$, and the thick solid curve is the topological charge parameter $A(T)^{1/4}$. The decay constants $f_\pi(T)$ and $f_{s\bar{s}}(T)$ are, respectively, the lower dashed and dash-dotted curves.

This behavior is followed closely by $\tilde{\chi}(T)$, and therefore also by the anomaly parameter $\beta_{\text{WV}}(T)$ [Eq. (11)]. This makes the mass matrix (10) diagonal immediately after $T = T_{\text{Ch}}$, which marks the abrupt onset of the NS-S scenario $M_{\eta'}(T) \rightarrow M_{s\bar{s}}(T)$, $M_\eta(T) \rightarrow M_\pi(T)$ [9].

In Eq. (13), \mathcal{C}_m denotes corrections of higher orders in small m_q , but it should not be neglected as $\mathcal{C}_m \neq 0$ is needed to have a finite χ_{YM} with Eqs. (12) and (13). They in turn give us the value \mathcal{C}_m at $T = 0$ in terms of the $q\bar{q}$ condensate and the YM topological susceptibility χ_{YM} . However, to the best of our knowledge, the functional form of \mathcal{C}_m is not known. Reference [9] thus tried various parametrizations covering reasonably possible T dependences of $\mathcal{C}_m(T)$, but this did not greatly affect the results for the T dependence of the masses in the η' - η complex.

An alternative to the WVR (6) is its generalization by Shore [13,14]. There, relations containing the masses of the pseudoscalar nonet mesons take into account that η and η' should have two decay constants each [42]. If one chooses to use the η_8 - η_0 basis, they are $f_\eta^8, f_{\eta'}^8, f_\eta^0, f_{\eta'}^0$, and can be equivalently expressed through purely octet and singlet decay constants (f_8, f_0) and two mixing angles (θ_8, θ_0). This may seem better suited for use with effective meson Lagrangians than with $q\bar{q}'$ substructure calculations starting from the (flavor-broken) nonet symmetry, such as ours. Nevertheless, Shore's approach was also adapted for the latter bound-state context, and successfully applied there (in particular, to our DS approach in the RLA [27]). This was thanks to the simplifying scheme of Feldmann, Kroll, and Stech (FKS) [43,44]. They showed that this “two mixing angles for four decay constants” formulation in the NS-S basis, although in principle equivalent to the η_8 - η_0 basis formulation, can in practice be simplified further to a one-mixing-angle scheme using plausible approximations based on the Okubo-Zweig-Iizuka (OZI) rule. The decay-constant mixing angles in this basis are mutually close, $\phi_S \approx \phi_{\text{NS}}$, and both are approximately equal to the state mixing angle ϕ rotating the NS-S basis states into the physical η and η' mesons,

$$\eta = \cos \phi \eta_{\text{NS}} - \sin \phi \eta_S, \quad \eta' = \sin \phi \eta_{\text{NS}} + \cos \phi \eta_S, \quad (14)$$

which diagonalizes the mass (squared) matrix (10).

So, Ref. [27] numerically solved Shore's equations (combined with the FKS approximation scheme) for meson masses for several dynamical DS bound-state models [24,34,35]. Then, Ref. [11] presented analytic solutions thereof, for the masses of η and η' and the state NS-S mixing angle ϕ . These are rather long but closed-form expressions in terms of nonanomalous meson masses M_π, M_K and their decay constants f_π, f_K , as well as f_{NS} and f_S (the decay constants of the unphysical η_{NS} and η_S), and, most notably, the full-QCD topological charge parameter A . This quantity (taken [13,14] from Di Vecchia and Veneziano [15]) plays the role of χ_{YM} in the WVR in the mass relations of Shore's

generalization. A will be considered in detail for the $T > 0$ extension, but now let us note that although Shore's generalization is in principle valid to all orders in $1/N_c$ [13,14], Shore himself took advantage of

$$A = \chi_{\text{YM}} + \mathcal{O}\left(\frac{1}{N_c}\right) \quad (\text{at } T = 0) \quad (15)$$

and approximated A (as we shall at $T = 0$) by the lattice result $\chi_{\text{YM}} = (0.191 \text{ GeV})^4$ [45].

Further, one should note that since the FKS scheme neglects OZI-violating contributions (that is, gluonium admixtures in η_{NS} and η_{S}) it is consistent to treat them as pure $q\bar{q}$ states, accessible by our BSE (2) in the RLA. Then $f_{\text{NS}} = f_{\pi}$, and $f_{\text{S}} = f_{s\bar{s}}$ (the decay constant of the aforementioned ‘‘auxiliary’’ RLA $s\bar{s}$ pseudoscalar). We calculate its mass $M_{s\bar{s}}$ with the BSE, but at $T = 0$ it can also be related to the measurable pion and kaon masses, $M_{s\bar{s}}^2 \approx 2M_K^2 - M_{\pi}^2$, due to Eq. (5). Similarly, $f_{s\bar{s}}$ can also be approximately expressed with these measurable quantities as $f_{s\bar{s}} \approx 2f_K - f_{\pi}$. Thus, after taking $A \approx \chi_{\text{YM}}$ from lattice data, Ref. [11] calculated the η - η' complex using both the model-calculated and the empirical M_{π} , M_K , f_{π} , and f_K in their analytic solutions. This serves as a check (independently of any model) of the soundness of our approach at $T = 0$.

The analytic solutions of Ref. [11] also lead to simple elements of the mass matrix (10),

$$M_{\text{NS}}^2 = M_{\pi}^2 + \frac{4A}{f_{\pi}^2}, \quad M_{\text{NS S}}^2 = \frac{2\sqrt{2}A}{f_{\pi}f_{s\bar{s}}}, \quad (16)$$

$$M_{\text{S}}^2 = M_{s\bar{s}}^2 + \frac{2A}{f_{s\bar{s}}^2}, \quad (17)$$

implying $X = f_{\pi}/f_{s\bar{s}}$, $M_{U_A(1)}^2 = 4A/f_{\pi}^2 + 2A/f_{s\bar{s}}^2$, and β_{Sho} in Eq. (11). The approximation $A = \chi_{\text{YM}}$ [Eq. (15)] with $\chi_{\text{YM}} = (0.191 \text{ GeV})^4$ from lattice data [45] then yields $M_{\eta'} = 997 \text{ MeV}$ and $M_{\eta} = 554 \text{ MeV}$ at $T = 0$.

Since the adopted DS model also enables the calculation of nonanomalous $q\bar{q}$ masses and decay constants for $T > 0$, the only thing still missing is the T dependence of the full-QCD topological charge parameter A , as $\chi_{\text{YM}}(T)$ is inadequate. But, A is used to express the QCD susceptibility χ through the ‘‘massive’’ condensates $\langle \bar{u}u \rangle$, $\langle \bar{d}d \rangle$, and $\langle \bar{s}s \rangle$, i.e., away from the chiral limit, in contrast to Eqs. (12) and (13) [see, e.g., Eq. (2.12) in Ref. [13]]. Its inverse (expressing A) thus also contains the $q\bar{q}$ condensates out of the chiral limit for all light flavors $q = u, d, s$,

$$A = \frac{\chi}{1 + \chi\left(\frac{1}{m_u\langle \bar{u}u \rangle} + \frac{1}{m_d\langle \bar{d}d \rangle} + \frac{1}{m_s\langle \bar{s}s \rangle}\right)}, \quad (18)$$

and so should χ in Eq. (18). That is, the light-quark expression for the QCD topological susceptibility in the

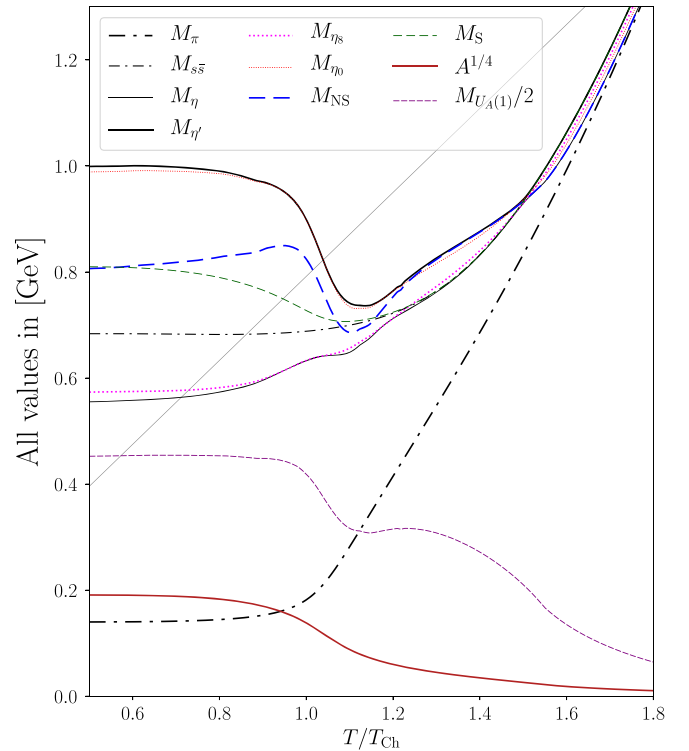


FIG. 3. T dependence, relative to T_{Ch} , of various η - η complex masses described in the text, the π mass (thick, dash-dotted curve) for reference, the halved (to maintain clarity) total $U_A(1)$ -anomaly-induced mass $\frac{1}{2}M_{U_A(1)}$ (short-dashed curve), and the topological charge parameter $A^{1/4}$ (solid curve). The straight line is 2 times the lowest fermion Matsubara frequency $2\pi T$.

context of Shore's approach should be expressed in terms of the current masses m_q multiplied by their respective condensates $\langle \bar{q}q \rangle$ realistically out of the chiral limit:

$$\chi = \frac{-1}{\frac{1}{m_u\langle \bar{u}u \rangle} + \frac{1}{m_d\langle \bar{d}d \rangle} + \frac{1}{m_s\langle \bar{s}s \rangle}} + C_m. \quad (19)$$

As before [9], the small and necessarily negative correction term C_m is found by assuming $A = \chi_{\text{YM}}$ at $T = 0$. This large- N_c approximation also easily recovers the LS relation (12): by approximating the realistically massive condensates with $\langle \bar{q}q \rangle_0$ everywhere in Eq. (18), the QCD topological charge parameter A reduces to $\tilde{\chi}$, justifying the conjecture of Ref. [9] that connects the $U_A(1)$ symmetry restoration with the chiral symmetry restoration.

This connection between the two symmetries is still present. However, with the massive condensates we also get a more realistic, crossover T dependence of the masses, depicted in Figs. 3 and 4, and presented in Sec. IV.

Figures 3 and 4 correspond to two variations of the unknown T dependence $C_m(T)$ of the correction term in Eq. (19). As in Ref. [9], the simplest *ansatz* is a constant, $C_m(T) = C_m(0)$, which is most reasonable for $T < T_{\text{Ch}}$, where the condensates [and thus also the leading term in

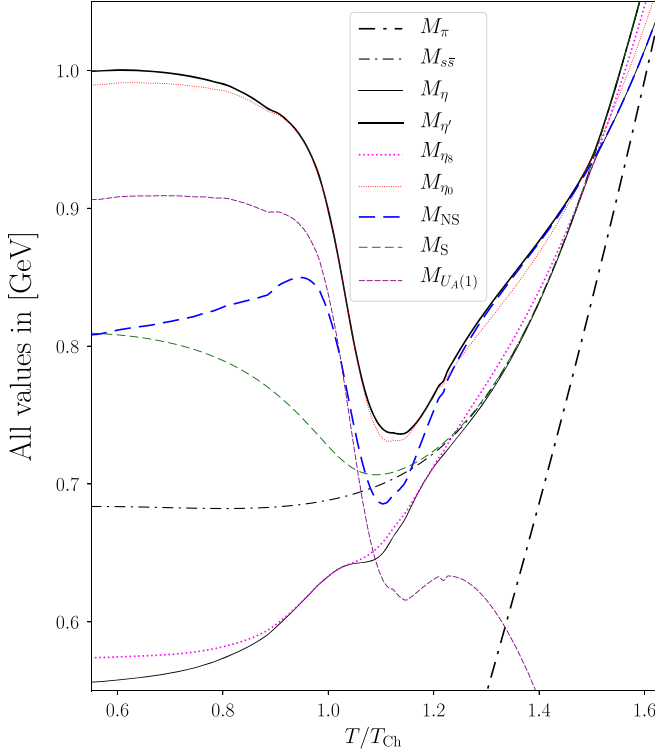


FIG. 4. T/T_{Ch} dependence of pseudoscalar meson masses zoomed to the area important for the η' - η complex, for the simplest Ansatz $C_m(T) = \text{constant} = C_m(0)$, which limits temperatures to $T \lesssim 1.6T_{\text{Ch}}$.

$\chi(T)$] change little. But above some higher T , the negative $C_m(0)$ —although initially much smaller in magnitude than the leading term—will make $\chi(T)$ [and therefore also $A(T)$] change sign. Concretely, this limiting T above which there is no meaningful description is found a little above $1.6T_{\text{Ch}}$.

For another, nonconstant $C_m(T)$ that would not have such a limiting temperature, we now have a lead from lattice data where the high- T asymptotic behavior of the QCD topological susceptibility has been found to be a power law, $\chi(T) \propto T^{-b}$ [46,47]. The high- T dependence of our model-calculated condensates is also (without fitting) such that the leading term of our $\chi(T)$ in Eq. (19) has a similar power-law behavior, with $b = 5.17$. Also, the values of our leading terms are, qualitatively, for all T roughly in the same ballpark as the lattice results [46,47]. We thus fit the quickly decreasing power-law $C_m(T)$ for high T by requiring that (i) this more or less rough consistency with lattice $\chi(T)$ values is preserved, (ii) the whole $\chi(T)$ has the high- T power-law dependence as the leading term (with $b = 5.17$), and (iii) $C_m(T)$ joins smoothly with the low- T value $C_m(0)$ determined from χ_{YM} at $T = 0$.

Our nonconstant choice of $C_m(T)$ yields the masses in Fig. 3 [and $\chi(T)$ and $A(T)$ in Fig. 2], but these results are very similar to the ones with $C_m(T) = C_m(0)$ (of course, only up to the limiting T a little above $1.6T_{\text{Ch}}$) in Fig. 4. Thus, Fig. 4 uses a different scale than Fig. 3, i.e., only the

mass interval between 0.55 and 1.05 GeV, so as to zoom in on the η - η' complex and better discern its various overlapping curves, including $M_{U_A(1)}(T)$.

The second choice of $C_m(T)$ enables in principle the calculation of $\chi(T)$ and $A(T)$ without any limiting T . Nevertheless, Fig. 3 does not reach higher than $T = 1.8T_{\text{Ch}}$, because the model chosen for the RLA part of our calculations seems to become unreliable at higher T 's: the mass eigenvalues seem increasingly too high, since they tend to cross the sum of the lowest $q + \bar{q}$ Matsubara frequencies. Fortunately, by $T/T_{\text{Ch}} = 1.8$ the asymptotic scenario for the anomaly has been reached, as we explain in the next section where we give a detailed description of all pertinent results at $T \geq 0$.

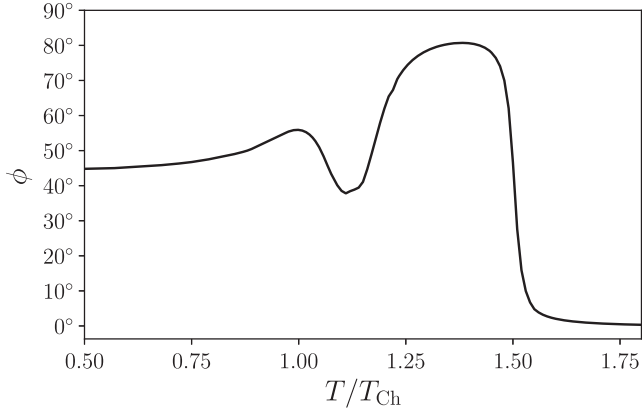
IV. RESULTS AT $T \geq 0$ IN DETAIL

Figure 2 shows how various magnitudes of current-quark masses m_q influence the T dependence and size of $q\bar{q}$ condensates $\langle \bar{q}q \rangle$ and pseudoscalar decay constants $f_{q\bar{q}}$ calculated in our adopted model. Defined, e.g., in Sec. II A of Ref. [24], it employs the parameter values $m_u = m_d \equiv m_l = 5.49$ MeV and $m_s = 115$ MeV.

For both condensates and decay constants, larger current-quark masses lead to larger “initial” (i.e., $T = 0$) magnitudes and, what is even more important for the present work, to smoother and slower falloffs with T . The magnitude of (the third root of) the strange-quark condensate is the top dash-dotted curve in Fig. 2. Its $T = 0$ value $|\langle \bar{s}s \rangle|^{1/3} = 238.81$ MeV remains almost unchanged until $T = T_{\text{Ch}}$, and falls below 200 MeV (i.e., by some 20%) only for $T \approx 1.5T_{\text{Ch}}$. On the other hand, the $T = 0$ value of the isosymmetric condensates of the lightest flavors, $\langle \bar{u}u \rangle = \langle \bar{d}d \rangle \equiv \langle \bar{l}l \rangle = (-218.69 \text{ MeV})^3$, is quite close to the chiral one, $\langle \bar{q}q \rangle_0 = (-216.25 \text{ MeV})^3$, showing how well the chiral limit works for u and d flavors in this respect. Still, the small current masses of u and d quarks are sufficient to lead to a very different T dependence of the lightest condensates, depicted by the dashed curve. It exhibits a typical smooth crossover behavior around $T = T_{\text{Ch}}$, and while the decrease is much more pronounced than in the case of $\langle \bar{s}s \rangle$, it differs qualitatively from the sharp decrease to zero exhibited by the chiral condensate [and thus also by the anomaly-related quantity $\tilde{\chi}(T)$ defined by the LS relation (12)].

The isosymmetric pion decay constant $f_\pi(T) \equiv f_{\bar{l}l}(T)$ is the lower dashed curve in Fig. 2, starting at $T = 0$ from our model-calculated value $f_\pi = 92$ MeV. It decreases rather quickly, in contrast to $f_{s\bar{s}}(T)$ [starting at $f_{s\bar{s}}(T = 0) = 119$ MeV], the decay constant of the unphysical RLA $\bar{s}s$ pseudoscalar. It exhibits a much “slower” T dependence, in accordance with the s -quark condensate $\langle \bar{s}s \rangle(T)$.

The behavior of $m_l \langle \bar{l}l \rangle(T)$ largely determines that of the full-QCD topological charge parameter $A(T)$, depicted in Fig. 2 by the thick solid curve, and in Fig. 3 by the solid curve: A is dominated by the lightest flavor, just like


 FIG. 5. Relative T dependence of the NS-S mixing angle $\phi(T)$.

χ and $\tilde{\chi}$, as shown by their related defining expressions (18)–(19) and (12)–(13).

The smooth, monotonic decrease of $A(T)$ after $T \sim 0.7T_{\text{Ch}}$ reflects the degree of gradual, crossover restoration of the $U_A(1)$ symmetry with T . How this is reflected in the masses in the η - η' complex also depends on the ratios of $A(T)$ with $f_\pi^2(T)$, $f_\pi f_{s\bar{s}}(T)$, and $f_{s\bar{s}}^2(T)$ in Eqs. (16) and (17). $M_{\text{NS}}^2 \propto A(T)/[f_\pi(T)f_{s\bar{s}}(T)]$ decreases comparably to $A(T)^{1/2}$, and $2A(T)/f_{s\bar{s}}(T)^2$ decreases even faster. Thus, $M_S(T)$ [Eq. (17)] monotonically becomes the anomaly-free $M_{s\bar{s}}(T)$ in basically the same way as in Ref. [9], except now this process is not completed at $T = T_{\text{Ch}}$ but rather [due to the $A(T)$ crossover] drawn out until $T \approx 1.15T_{\text{Ch}}$.

In contrast, $\beta_{\text{Sho}}(T) = 2A(T)/f_\pi^2(T)$ even grows for $T < 0.95T_{\text{Ch}}$ and $1.15T_{\text{Ch}} \lesssim T \lesssim 1.25T_{\text{Ch}}$. By making $M_{\text{NS}}(T) > M_S(T)$ it causes the increase of the mixing angle ϕ (look at Figs. 3–5 together). Note that this makes the η_8 - η_0 -state mixing angle $\theta(\approx \phi - 55^\circ)$ less negative, i.e., closer to zero, and brings η_0 and η_8 in an even better agreement with, respectively, η' and η , than at $T = 0$.

These two limited increases of $A(T)/f_\pi^2(T)$ may be model dependent and are not important, but what is systematic and thus important is that the “light” decay constant $f_\pi(T)$ makes $\sqrt{A(T)/f_\pi^2(T)}$ more resilient to T than not only $A(T)^{1/4}$ itself, but also other anomalous mass contributions in Eqs. (16) and (17).

Indeed, $\beta_{\text{Sho}}(T) = 2A(T)/f_\pi^2(T)$ decreases only after $T \approx 0.95T_{\text{Ch}}$ (contributing over a half of the η' mass decrease), and then again increases somewhat after $T \approx 1.15T_{\text{Ch}}$, to start definitively decreasing only after $T \approx 1.25T_{\text{Ch}}$, but even then slower than other anomalous contributions. This makes $M_{\text{NS}}(T)$ larger enough than $M_S(T)$ to increase $\phi(T)$ around 80° , and keep it there up to $T \sim 1.5T_{\text{Ch}}$ (see Fig. 5).

This explains how the masses of the physical mesons η' and η (thick and thin solid curves in Figs. 3 and 4),

$$M_{\eta'(\eta)}^2 = \frac{M_{\text{NS}}^2 + M_S^2}{2} + (-) \sqrt{\left(\frac{M_{\text{NS}}^2 - M_S^2}{2}\right)^2 + M_{\text{NS}}^4}, \quad (20)$$

exhibit the decrease of the mass of the heavier partner η' which is almost as strong as in the case [9] of the abrupt disappearance of the anomaly contribution, while on the contrary the lighter partner η now shows no sign of a decrease in mass around $T = T_{\text{Ch}}$, let alone an abrupt degeneracy with the pion. The latter happens in the case with the sharp phase transition because the fast disappearance of the *whole* $M_{U_A(1)}$ around T_{Ch} can be accommodated only by a sharp change of the state mixing ($\phi \rightarrow 0$) to fulfill the asymptotic NS-S scenario immediately after T_{Ch} . (See in particular Fig. 2 in Ref. [9]. Note that in our approach $M_{\eta'}(T)$ cannot decrease by much more than a third of $M_{U_A(1)}$, since the RLA $M_{s\bar{s}}(T)$ is the lower limit of $M_{\eta'}(T)$ both in Ref. [9] and here.)

In the present crossover case, however, $T = T_{\text{Ch}}$ does not mark a drastic change in the mixing of the isoscalar states, but η' stays mostly η_0 and η stays mostly η_8 . Then, $\Delta M_{\eta_8}^2 = 4A(1/f_\pi - 1/f_{s\bar{s}})^2/3$ [from Eq. (8)] can serve as a compact illustration of how for the lighter partner η [with (–) in Eq. (20)] anomalous contributions cancel to a large extent. Thus, the mass of η behaves mostly like the masses of other $q\bar{q}'$ (almost-)Goldstone bosons after losing their chiral protection at T_{Ch} : it just suffers the thermal increase towards $2\pi T$.

Nevertheless, in $M_{\eta'}$ [Eq. (20)], the anomalous contributions from Eqs. (16) and (17) are all added together. The *partial* restoration of $U_A(1)$ symmetry around T_{Ch} , where around a third of the total $U_A(1)$ -anomalous mass $M_{U_A(1)}$ goes away, is consumed almost entirely by the decrease of the η' mass over the crossover.

After $T \approx 1.15T_{\text{Ch}}$, $M_{\eta'}(T)$ starts rising again, but this is expected since after $T \approx T_{\text{Ch}}$ light pseudoscalar mesons start their thermal increase towards $2\pi T$, which is twice the lowest Matsubara frequency of the free quark and antiquark. This rather steep joint increase brings all of the mass curves $M_P(T)$ quite close after $T \sim 1.5T_{\text{Ch}}$. The kaon mass $M_K(T)$ is not shown in Figs. 3 and 4 to maintain clarity by avoiding crowded curves, but at this temperature of the characteristic η - η' anticrossing, $M_K(T)$ is roughly in between $M_\pi(T)$ and the η mass, and is soon crossed by $M_\eta(T)$ which tends to become degenerate with $M_\pi(T)$ (as detailed below).

The rest of $M_{U_A(1)}(T)$ [melting as $2\sqrt{A(T)}/f_\pi(T)$] under $1.5T_{\text{Ch}}$ is sufficiently large to keep $M_{\text{NS}}(T) > M_S(T)$ and $\phi \approx 80^\circ$. So a large ϕ makes θ positive, but not very far from zero, so that there we still have $\eta' \approx \eta_0$ and $\eta \approx \eta_8$. This is also a fairly good approximation for $T > 1.25T_{\text{Ch}}$, but there an even better approximation is $\eta' \approx \eta_{\text{NS}}$, $M_{\eta'}(T) \approx M_{\text{NS}}(T)$ and $\eta \approx \eta_S$, $M_\eta(T) \approx M_S(T)$. Finally, Eq. (20) enforces anticrossing at $T \approx 1.5T_{\text{Ch}}$ when the anomalous mass contribution becomes so small that $M_{\text{NS}}(T) = M_S(T)$. $M_{\text{NS}}(T)$ and $M_S(T)$ switch, and after this the η - η' complex enters the NS-S asymptotic regime of the vanishing anomaly influence: $M_{\eta'}(T) \rightarrow M_S(T) \rightarrow M_{s\bar{s}}(T)$, $M_\eta(T) \rightarrow M_{\text{NS}}(T) \rightarrow M_\pi(T)$, and $\phi(T) \rightarrow 0$.

V. SUMMARY, DISCUSSION, AND CONCLUSIONS

We have studied the temperature dependence of the masses in the $\eta' - \eta$ complex in the regime of the crossover restoration of chiral and $U_A(1)$ symmetry. We relied on the approach of Ref. [11], which demonstrated the soundness of the approximate way in which the $U_A(1)$ -anomaly effects on pseudoscalar masses were introduced and combined [24,27,34–37] with chirally well-behaved DS RLA calculations in order to study η' and η . For $T = 0$, this was demonstrated [11] model independently, with the only inputs being the experimental values of pion and kaon masses and decay constants, and the lattice value of the YM topological susceptibility. However, at $T > 0$ dynamical models are still needed to generate the temperature dependence of nonanomalous quantities through DS RLA calculations, and in this paper we used the same chirally correct and phenomenologically well-tested model as in numerous earlier $T \geq 0$ studies (see, e.g., Refs. [9,24,31] and references therein).

Following Ref. [11], we assumed that the anomalous contribution to the masses is related to the full-QCD topological charge parameter (18), which contains the massive quark condensates. They give us the chiral crossover behavior for high T . This is crucial, since lattice QCD calculations have established that for the physical quark masses, the restoration of the chiral symmetry occurs as a crossover (see, e.g., Refs. [29,48,49] and references therein) characterized by the pseudocritical transition temperature T_{Ch} .

Nevertheless, what happens with the $U_A(1)$ restoration is still not clear [48,50–52]. Whereas, e.g., Ref. [29] found its breaking as high as $T \sim 1.5T_{\text{Ch}}$, Ref. [53] found that above the critical temperature $U_A(1)$ is restored *in the chiral limit*, and the JLQCD Collaboration [52] discussed the possible disappearance of the $U_A(1)$ anomaly and pointed out the tight connection with the chiral symmetry restoration. Hence, there is a need to clarify “*if, how (much), and when*” [48] $U_A(1)$ symmetry is restored. In such a situation, we believe instructive insight can be found in our study of how an anomaly-generated mass influences the η - η' complex, although this study is not done at the microscopic level.

Since the JLQCD Collaboration [52] has recently stressed that the chiral symmetry breaking and $U_A(1)$ anomaly are tied for quark bilinear operators (as, e.g., in our Eqs. (12), (13), (18) and (19), where the chiral symmetry breaking drives the $U_A(1)$ one through $q\bar{q}$ condensates), we again recall how Ref. [11] provided support for the earlier proposal of Ref. [9] relating DChSB to the $U_A(1)$ -anomalous mass contributions in the η' - η complex. This adds to the motivation to determine the full-QCD topological charge parameter (18) on the lattice from simulations in full QCD with massive, dynamical quarks [besides the original motivation [13,14] to remove the systematic $\mathcal{O}(1/N_c)$ uncertainty of Eq. (15)]. More importantly, this connects the $U_A(1)$ symmetry breaking and restoration to those of chiral

symmetry. It connects them in basically the same way in both Refs. [9,11] (and here), except that the full-QCD topological charge parameter (18) enables the crossover $U_A(1)$ restoration by allowing the use of the massive quark condensates. But, if the chiral condensate (i.e., of *massless* quarks) is used to extend the approach of Ref. [11] to finite temperatures, the $T > 0$ results are, in essence, very similar to those of Ref. [9]: the quick chiral phase transition leads to quick $U_A(1)$ symmetry restoration at T_{Ch} (consistent with Ref. [53]), which causes not only the empirically supported [5] decrease of the η' mass but also an even larger η mass decrease; if $M_{U_A(1)}^2(T) \propto \beta(T) \rightarrow 0$ abruptly when $T \rightarrow T_{\text{Ch}}$, Eq. (10) mandates that $M_{\eta}(T \rightarrow T_{\text{Ch}}) \rightarrow M_{\pi}(T_{\text{Ch}})$ equally abruptly (as in Ref. [9]). However, no experimental indication for this has ever been seen, although this is a more drastic decrease than for the η' meson.

The present paper predicts a more realistic behavior of $M_{\eta}(T)$ thanks to the smooth chiral restoration, which in turn yields the smooth, partial $U_A(1)$ symmetry restoration (as far as the masses are concerned) making various actors in the η - η' complex behave quite differently from the abrupt phase transition (such as that in Ref. [9]). In particular, the η mass is now not predicted to decrease, but to only increase after $T \approx T_{\text{Ch}}$, just like the masses of other (almost-) Goldstone pseudoscalars, which are free of the $U_A(1)$ anomaly influence. Similarly to $T = 0$, η agrees rather well with the $SU(3)$ flavor state η_8 until the anticrossing temperature, which marks the beginning of the asymptotic NS-S regime, where the anomalous mass contributions become increasingly negligible and $\eta \rightarrow \eta_{\text{NS}}$.

In contrast to η , the η' mass $M_{\eta'}(T)$ does decrease similarly to the case of the sharp phase transition, where its lower limit [namely, $M_{s\bar{s}}(T)$] is reached at T_{Ch} [9]. Now, $M_{\eta'}(T)$ at its minimum (which is only around $1.13T_{\text{Ch}}$ because of the rather extended crossover) is some 20 to 30 MeV above $M_{s\bar{s}}(T)$, after which they both start to grow appreciably, and $M_{\eta'}(T)$ is reasonably approximated by $M_{\eta_0}(T)$ up to the anticrossing. The effective restoration of $U_A(1)$ regarding the η - η' masses only occurs beyond the anticrossing at $T \approx 1.5T_{\text{Ch}}$, in the sense of reaching the asymptotic regime $M_{\eta'}(T) \rightarrow M_{s\bar{s}}(T)$. Another, less qualitatively illustrative but more quantitative criterion for the degree of $U_A(1)$ restoration is that there, at $T \approx 1.5T_{\text{Ch}}$, $M_{U_A(1)}$ is still slightly above 40%, and at $T \approx 1.8T_{\text{Ch}}$ still around 14% of its $T = 0$ value. Thus, the decrease to the minimum of $M_{\eta'}(T)$ around $1.13T_{\text{Ch}}$ in any case signals only a partial $U_A(1)$ restoration.

This $M_{\eta'}(T)$ decrease is around 250 MeV, which is consistent with the current empirical evidence claiming that it is at least 200 MeV [5]. For comparison with some other approaches that explore the interplay of the chiral phase transition and axial anomaly, note that the η' mass decrease around 150 MeV is found in the functional renormalization group approach [54]. A very

recent analysis within the framework of the $U(3)$ chiral perturbation theory found that the (small) increase of the masses of π , K , and η after around $T \sim 120$ MeV, is accompanied by the decrease of the η' mass, but only by some 15 MeV [55].

Admittedly, the crossover transition leaves more space for model dependence, since some model changes that would make the crossover even smoother would reduce our η' mass decrease. Nevertheless, there are also changes that would make it steeper, and those may, for example, help $M_{\eta'}(T)$ saturate the $M_{s\bar{s}}(T)$ limit. Exploring such model dependences, as well as attempts to further reduce them at $T > 0$ by including more lattice QCD results, must be relegated to future work. However, here we can already note a motivation for varying the presently isosymmetric *model* current u - and d -quark mass of 5.49 MeV. Since it is essentially a phenomenological model parameter, it cannot be quite unambiguously and precisely related to the somewhat lower Particle Data

Group values $m_u = 2.2^{+0.5}_{-0.4}$ MeV and $m_d = 4.70^{+0.5}_{-0.3}$ MeV [56]. Still, their ratio $m_u/m_d = 0.48^{+0.07}_{-0.08}$ is quite instructive in the present context, since the QCD topological susceptibility χ [Eq. (19)] and charge parameter A [Eq. (18)] contain the current-quark masses in the form of harmonic averages of $m_q \langle \bar{q}q \rangle$ ($q = u, d, s$). Since a harmonic average is dominated by its smallest argument, our χ and A are dominated by the lightest flavor, providing the motivation to venture beyond the precision of the isospin limit and in future work explore the maximal isospin violation scenario [57] within the present treatment of the η - η' complex.

ACKNOWLEDGMENTS

This work was supported in part by the Croatian Science Foundation under the Project No. 8799, and by STSM grants from COST Actions CA15213 THOR and CA16214 PHAROS. D. Kl. thanks T. Csörgő and D. Blaschke for many helpful discussions.

-
- [1] Y. Akiba *et al.*, [arXiv:1502.02730](https://arxiv.org/abs/1502.02730).
- [2] A. Dainese *et al.*, *Frascati Phys. Ser.* **62** (2016).
- [3] S. S. Adler *et al.* (PHENIX Collaboration), *Phys. Rev. Lett.* **93**, 152302 (2004).
- [4] J. Adams *et al.* (STAR Collaboration), *Phys. Rev. C* **71**, 044906 (2005).
- [5] T. Csörgő, R. Vertesi, and J. Sziklai, *Phys. Rev. Lett.* **105**, 182301 (2010); R. Vertesi, T. Csörgő, and J. Sziklai, *Phys. Rev. C* **83**, 054903 (2011); M. Vargyas, T. Csörgő, and R. Vertesi, *Central Eur. J. Phys.* **11**, 553 (2013).
- [6] J. I. Kapusta, D. Kharzeev, and L. D. McLerran, *Phys. Rev. D* **53**, 5028 (1996).
- [7] A. Adare *et al.* (PHENIX Collaboration), *Phys. Rev. C* **97**, 064911 (2018).
- [8] T. Csörgő, HBT overview—with an emphasis on multiparticle correlation, in *XLVII Internat. Symposium on Multiparticle Dynamics (ISMD2017), Tlaxcala, Mexico* (unpublished), <https://indico.nucleares.unam.mx/event/1180/session/22/contribution/106/material/slides/5.pdf>.
- [9] S. Benić, D. Horvatić, D. Kekez, and D. Klabučar, *Phys. Rev. D* **84**, 016006 (2011).
- [10] H. Leutwyler and A. V. Smilga, *Phys. Rev. D* **46**, 5607 (1992).
- [11] S. Benić, D. Horvatić, D. Kekez, and D. Klabučar, *Phys. Lett. B* **738**, 113 (2014).
- [12] C. Aidala *et al.* (PHENIX Collaboration), *Phys. Rev. C* **98**, 054903 (2018).
- [13] G. M. Shore, *Nucl. Phys.* **B744**, 34 (2006).
- [14] G. M. Shore, *Lect. Notes Phys.* **737**, 235 (2008); *Nucl. Phys.* **B569**, 107 (2000).
- [15] P. Di Vecchia and G. Veneziano, *Nucl. Phys.* **B171**, 253 (1980).
- [16] R. Alkofer and L. von Smekal, *Phys. Rep.* **353**, 281 (2001).
- [17] C. D. Roberts and S. M. Schmidt, *Prog. Part. Nucl. Phys.* **45**, S1 (2000).
- [18] A. Höll, C. D. Roberts, and S. V. Wright, [arXiv:nucl-th/0601071](https://arxiv.org/abs/nucl-th/0601071).
- [19] C. S. Fischer, *J. Phys. G* **32**, R253 (2006).
- [20] G. Eichmann, R. Williams, R. Alkofer, and M. Vujanović, *Phys. Rev. D* **89**, 105014 (2014).
- [21] D. Binosi, L. Chang, J. Papavassiliou, S. X. Qin, and C. D. Roberts, *Phys. Rev. D* **93**, 096010 (2016).
- [22] S. x. Qin, *Few Body Syst.* **57**, 1059 (2016).
- [23] D. Blaschke, G. Bureau, Y. L. Kalinovsky, P. Maris, and P. C. Tandy, *Int. J. Mod. Phys. A* **16**, 2267 (2001).
- [24] D. Horvatić, D. Klabučar, and A. E. Radzhabov, *Phys. Rev. D* **76**, 096009 (2007).
- [25] D. Blaschke, Y. L. Kalinovsky, A. E. Radzhabov, and M. K. Volkov, *Phys. Part. Nucl. Lett.* **3**, 327 (2006).
- [26] D. Horvatić, D. Blaschke, D. Klabučar, and A. E. Radzhabov, *Phys. Part. Nucl.* **39**, 1033 (2008).
- [27] D. Horvatić, D. Blaschke, Y. Kalinovsky, D. Kekez, and D. Klabučar, *Eur. Phys. J. A* **38**, 257 (2008).
- [28] A. Bazavov *et al.*, *Phys. Rev. D* **85**, 054503 (2012).
- [29] V. Dick, F. Karsch, E. Laermann, S. Mukherjee, and S. Sharma, *Phys. Rev. D* **91**, 094504 (2015).
- [30] A. Bazavov *et al.*, *Phys. Rev. D* **95**, 054504 (2017).
- [31] D. Horvatić, D. Blaschke, D. Klabučar, and O. Kaczmarek, *Phys. Rev. D* **84**, 016005 (2011).
- [32] E. Witten, *Nucl. Phys.* **B156**, 269 (1979).
- [33] G. Veneziano, *Nucl. Phys.* **B159**, 213 (1979).
- [34] D. Kekez, D. Klabučar, and M. D. Scadron, *J. Phys. G* **26**, 1335 (2000).
- [35] D. Kekez and D. Klabučar, *Phys. Rev. D* **73**, 036002 (2006).
- [36] D. Klabučar and D. Kekez, *Phys. Rev. D* **58**, 096003 (1998).

- [37] D. Kekez and D. Klabučar, *Phys. Rev. D* **65**, 057901 (2002).
- [38] M. S. Bhagwat, L. Chang, Y. X. Liu, C. D. Roberts, and P. C. Tandy, *Phys. Rev. C* **76**, 045203 (2007).
- [39] R. Alkofer, C. S. Fischer, and R. Williams, *Eur. Phys. J. A* **38**, 53 (2008).
- [40] F. J. Gilman and R. Kauffman, *Phys. Rev. D* **36**, 2761 (1987); **37**, 3348(E) (1988).
- [41] S. Dürr, *Nucl. Phys.* **B611**, 281 (2001).
- [42] See, e.g., the extensive review [43], or the Appendix in Ref. [36].
- [43] T. Feldmann, *Int. J. Mod. Phys. A* **15**, 159 (2000).
- [44] T. Feldmann, P. Kroll, and B. Stech, *Phys. Rev. D* **58**, 114006 (1998); *Phys. Lett. B* **449**, 339 (1999).
- [45] L. Del Debbio, L. Giusti, and C. Pica, *Phys. Rev. Lett.* **94**, 032003 (2005).
- [46] P. Petreczky, H. P. Schadler, and S. Sharma, *Phys. Lett. B* **762**, 498 (2016).
- [47] S. Borsanyi *et al.*, *Nature (London)* **539**, 69 (2016).
- [48] S. Aoki, H. Fukaya, and Y. Taniguchi, *Phys. Rev. D* **86**, 114512 (2012).
- [49] M. I. Buchoff *et al.*, *Phys. Rev. D* **89**, 054514 (2014).
- [50] S. Sharma (HotQCD Collaboration), arXiv:1801.08500.
- [51] F. Burger, E. M. Ilgenfritz, M. P. Lombardo, and A. Trunin, *Phys. Rev. D* **98**, 094501 (2018).
- [52] H. Fukaya (JLQCD Collaboration), *EPJ Web Conf.* **175**, 01012 (2018).
- [53] A. Tomiya, G. Cossu, S. Aoki, H. Fukaya, S. Hashimoto, T. Kaneko, and J. Noaki, *Phys. Rev. D* **96**, 034509 (2017); **96**, 079902(E) (2017).
- [54] M. Mitter and B. J. Schaefer, *Phys. Rev. D* **89**, 054027 (2014).
- [55] X. W. Gu, C. G. Duan, and Z. H. Guo, *Phys. Rev. D* **98**, 034007 (2018).
- [56] M. Tanabashi *et al.* (Particle Data Group), *Phys. Rev. D* **98**, 030001 (2018).
- [57] D. Kharzeev, R. D. Pisarski, and M. H. G. Tytgat, *Phys. Rev. Lett.* **81**, 512 (1998).